NATIONAL ADVISORY COMMITTEE FOR AERONAUTICS

TECHNICAL NOTE 3602

LABORATORY INVESTIGATION OF AN AUTOPILOT UTILIZING A MECHANICAL LINKAGE WITH A DEAD SPOT TO OBTAIN AN EFFECTIVE RATE SIGNAL

By Ernest C. Seaberg

Langley Aeronautical Laboratory
Langley Field, Va.

Washington
December 1955

NATIONAL ADVISORY COMMITTEE FOR AERONAUTICS

TECHNICAL NOTE 3602

LABORATORY INVESTIGATION OF AN AUTOPILOT UTILIZING A MECHANICAL LINKAGE WITH A DEAD SPOT TO OBTAIN AN EFFECTIVE RATE SIGNAL[1]

By Ernest C. Seaberg

SUMMARY

The roll automatic pilot investigated operates on a nonlinear principle, termed the frontlash principle, whereby a dead spot is incorporated in the servomotor feedback linkage to obtain an effective rate signal by reducing the phase lag of the servomotor. By application of the frontlash principle, the servomotor feedback linkage improves the servomotor phase response in a manner similar to that which would be obtained with the use of a rate gyroscope. However, the servomotor travel resulting from a given position-gyroscope displacement is decreased when the frontlash feedback linkage is used. Although the present application was for a roll automatic pilot, its application to other control systems appears feasible.

The results of this investigation indicate that the frontlash automatic pilot has promise as a pilotless-aircraft stabilization system. Laboratory tests of the system conducted on a roll simulator show that, in a certain range of simulated aerodynamic parameters, the nonlinear frontlash automatic pilot has a higher degree of stability than a comparable linear system. However, the transition from a stable to an unstable autopilot-aircraft combination appears to be more rapid with the nonlinear system. The results and applications in connection with the roll-simulator tests indicate that there are limitations in applying linear methods of theoretical analysis to systems having nonlinear components.

INTRODUCTION

As part of the general research program for testing various means of automatic stabilization, the Pilotless Aircraft Research Division of the Langley Aeronautical Laboratory has been conducting an investigation of various autopilot systems. Since this general research program is not limited to linear systems, an autopilot was designed to operate on

---

[1]Supersedes declassified NACA RM L9F15a.

a nonlinear principle, termed the frontlash principle, which employs a dead spot in the feedback linkage between the servomotor and the gyroscope base reference as a means of obtaining a leading control signal. The design of the autopilot is based on reference 1 and the purpose of this investigation is to determine the effect of frontlash on the amplitude and phase responses of the system. Roll-simulator tests of the frontlash autopilot were also conducted in the Instrument Research Division of the Langley Aeronautical Laboratory in order to confirm the possibility of stabilization of pilotless aircraft with this type of automatic pilot, and an attempt to bracket the useable range of this autopilot has been made by plotting the degree of stability as a function of the aerodynamic parameters.

SYMBOLS

δ servomotor movement, in.

θ oscillating-table displacement, deg

K control-amplitude ratio, $K = \frac{\delta}{\theta}$, in./deg

ϵ phase angle, deg (positive value indicates lead of δ ahead of θ)

ω angular frequency of oscillation, radians/sec

δ_a total aileron displacement, deg

ϕ angle of roll-simulator displacement, deg

$\dot{\phi}$ rolling angular velocity, $d\phi/dt$, radians/sec

L_{δ_a} rolling moment due to aileron deflection, $\partial L/\partial \delta_a$, ft-lb/radian/sec

$L_{\dot{\phi}}$ damping moment due to rolling velocity, $\partial L/\partial \dot{\phi}$, ft-lb/radian

I_x moment of inertia about longitudinal body axis, slug-ft^2

SC stability coefficient, a measure of degree of stability as defined in reference 2. (Value of this coefficient is unity for a highly damped (dead-beat) oscillation, zero for a steady-state oscillation, and negative for an unstable oscillation. Inset in fig. 14 shows method used to evaluate stability coefficient.)

a_n amplitude peaks in transient response used in defining stability coefficient (fig. 14)

L rolling moment, ft-lb

t time, sec

APPARATUS

Autopilot

The frontlash autopilot system used in this investigation consists of the two-gimbal air-driven displacement gyroscope from a German V-1 autopilot and a Jack & Heintz pneumatic servomotor (hereinafter to be referred to as servo).

The system operates as follows: In the case of an airframe being displaced about the gyro axis, an air jet, which is linked to the outer gimbal of the gyroscope by means of a cam, is directed towards either of two pickoff holes, which are connected to a 0.025-inch phosphor-bronze diaphragm by rubber tubes. This diaphragm is linked to the slide valve on the servo in such a manner that a differential pressure on the diaphragm actuates the slide valve which, in turn, causes movement of the servo piston for corrective control. A block diagram of the autopilot system is shown in figure 1. The autopilot also utilizes a mechanical feedback linkage between the servo piston and the jet pickoffs, which are capable of linear movement in the plane of jet rotation, as a means of effectively changing the gyro base reference. Dead spot for obtaining a leading control signal was incorporated in this feedback linkage by two methods and the results of tests on each were analyzed.

The first method of building dead spot into the system is shown in figure 2(a), where a dead spot of 0.021 inch is obtained by employing a simple loose link, and the static variation of servo position with oscillating-table displacement for a system of this type is shown in figure 2(b). The second method utilized a tension-compression spring and adjustable stops to obtain dead spot in the feedback linkage, as shown in figure 3(a). The relation between servo position and oscillating-table displacement for the spring system under static conditions is shown as a plot of δ against θ in figure 3(b). Although the curves contained in figures 2(b) and 3(b) show the static relation between δ and θ, different relations are obtained under dynamic conditions. Photographs of the two frontlash autopilot systems are shown in figure 4.

Equipment

An oscillating table capable of producing sinusoidal oscillations up to 5 cycles per second and with amplitude adjustments up to $\pm 15^{\circ}$ was used to obtain data for the amplitude- and phase-response tests. Position recorders were attached to the table and to the servo in order to record table motion and servo position as functions of time.

An electro-mechanical roll simulator was used to approximate the value of the frontlash autopilot as a means of pilotless-aircraft stabilization. With this instrument it is possible to estimate the stability characteristics of an autopilot-aircraft combination in roll. The automatic pilot is mounted in a cradle which simulates the combined behavior of an aircraft and automatic pilot when acted on by specific values of the following aerodynamic parameters:

$L\delta_a$ rolling moment due to aileron deflection

$L\dot{\phi}$ damping moment due to rolling velocity

I_x moment of inertia about the longitudinal body axis

RESULTS AND DISCUSSION

Preliminary Considerations

Preliminary tests were conducted to determine the effect of the following components on the amplitude and phase responses of the autopilot system:

Jet-pressure setting.- The magnitude of the jet pressure is limited because too high a jet pressure causes a high-frequency servo hunting oscillation at zero gyroscope reference attitude. However, if the jet pressure is too low, the servo piston travel, which varies with the magnitude of the jet pressure, will not be sufficient to move the feedback linkage through the dead spot at low values of table-oscillation amplitude. During this condition the lead sense of the system is ineffective because the jet pickoffs do not move. It seems desirable to have the jet pressure high enough to make the amplitude of table oscillation at which the frontlash is not effective in the order of $\pm 1^\circ$. On this basis, the jet-pressure settings obtained for this investigation were 3.5 psi for the loose-link system and 3 psi for the spring system. Figure 5 shows the variation in the loose-link-system servo response between a jet pressure of 1.5 and 3.5 psi. Although the response is more erratic, the higher jet pressure is desirable because the servo motion appears to lead the table motion at 3.5 psi.

Dead-spot size.- A high-frequency hunting oscillation at zero gyroscope reference attitude also results from too great a dead spot. However, in order to get the maximum effect from the dead spot, it is desirable that it be as large as possible. Using the values of jet pressure (3.5 and 3 psi) given in the preceding paragraph, the sizes of

dead spot at which this high-frequency oscillation started were 0.03 (±0.005) and 0.025 (±0.005) inch for the loose-link and spring system, respectively.

Bell-crank pivot point.- The bell-crank pivot point can be varied by moving the pivot bolt to the different holes in the bell crank which can be seen in figure 4. The range of pivot ratios investigated was as follows:

Loose-link system	3.86 to 14.9
Spring system	2.88 to 9.33

However, the position of the pivot point in these ranges did not seem to affect the response of the servo to the extent that it was affected by the jet pressure and the dead-spot size.

Jet-pickoff damping.- Some damping was imposed on the jet-pickoff motion by using an adjustable spring pressure to produce a variable amount of friction on the block containing the pickoff holes. This arrangement made it possible to use larger dead spots and jet pressures.

The results of the preliminary investigation on the foregoing components indicated that the combination of a dead spot of 0.021 inch with a jet pressure of 3.5 psi for the loose-link system and a dead spot of 0.016 inch with a jet pressure of 3 psi for the spring system would yield the best autopilot response characteristics and therefore these values were used for the amplitude- and phase-response analyses. The position of the bell-crank pivot point, which corresponded most favorably with these values, is shown in figures 2(a) and 3(a).

Autopilot Amplitude and Phase Response

The amplitude- and phase-response curves were obtained from a graphical analysis of the oscillating-table records, whereby the servo motion is approximated by an equivalent sine wave, as defined in reference 3. Using this method, the amplitude and phase responses were measured for table-oscillation frequencies of 0 to 5 cycles per second and for a range of table-oscillation amplitudes of ±1° to ±11°.

The German V-1 displacement gyroscope was first tested without dead spot by disconnecting the servo feedback linkage and fixing the position of the jet-pickoff block. Figure 6 gives the response of the autopilot system without dead spot to table-oscillation amplitudes of ±3.11° and ±7.34° with a jet pressure of 3.5 psi. The response curves contained in this figure will serve as a comparative basis for

the results of the tests using dead spot in the feedback linkage from the servo to the jet pickoffs.

Loose-link system.- The amplitude and phase responses of the loose-link system with a dead spot of 0.021 inch and a jet pressure of 3.5 psi are presented in figure 7 for the range of table amplitudes and frequencies. It can be seen that, except for an amplitude of $\pm 1.21^{\circ}$ where the servo travel is not sufficient to move the feedback linkage through the dead spot, the phase response has improved to the extent that the servo motion leads the table motion at the lower frequencies, and at approximately 5 cycles per second the servo lag is in the order of 10° or less as compared to a lag of 50° or 60° at the corresponding frequency without the loose link, figure 6. An examination of the control-amplitude-ratio curves in figure 7 indicates that a decrease in servo effectiveness accompanies the use of the loose-link system. It was also noted that the use of this type of feedback linkage restricted the servo movement to a certain maximum displacement, depending on the jet-pressure setting. For a jet pressure of 3.5 psi, the servo movement was limited to approximately 60 percent of its maximum throw regardless of the oscillating-table amplitude or frequency.

Spring system.- The use of a spring and adjustable stops in the linkage from the servo to the jet pickoffs was devised as a means of allowing the servo motion to continue after the jet pickoffs have moved through the dead spot. This arrangement made it possible to obtain full servo travel at extreme oscillating-table amplitudes. The amplitude and phase responses of this system with a dead spot of 0.016 inch and a jet pressure of 3 psi are presented in figure 8 for the range of table amplitudes and frequencies. The amplitude-response curves indicate that the servo effectiveness is about the same as for the loose-link system, although a somewhat smaller jet pressure was used.

In general, the spring-system phase response shows considerable improvement over a system without dead spot, although it is not quite as much as that obtained with the loose-link system. At an amplitude of $\pm 1.18^{\circ}$, however, the phase response does not appear to drop off as sharply as at the corresponding amplitude with the loose-link system. An explanation for this is that, although the servo motion is not sufficient to move the feedback linkage through the dead spot at this low amplitude, there is some follow-up motion of the jet pickoffs due to the tension-compression spring link between the bell crank and the pickoff block.

The phase-response curve at an amplitude of $\pm 2.92^{\circ}$ shows lead in the order of 40° to 50° at the higher frequencies. A rigorous explanation for this result is not known because the system is nonlinear. However, the pictorial representation of typical response curves at an

amplitude of ±2.92°, presented in figure 9, shows that at a low frequency the servo response is nonsinusoidal and becomes smoother and loses its lagging component as the frequency increases.

A presentation of the type of response obtained for a table-oscillating frequency of 2 cycles per second using the spring system is given in figure 10. The curves of this figure show typical examples of the nonsinusoidal servo response obtained because of the nonlinearities of this system. However, at amplitudes above ±3°, except for a slight reversal of servo piston travel caused by the movement of the jet pickoffs, the servo response appears to be proportional to and approximately in phase with the oscillating-table motion.

Roll-Simulator Tests

The test setup for the roll-simulator tests is shown in figure 11. With the use of this equipment it is possible to simulate the aerodynamic derivatives and record the closed-loop transient response of an aircraft-autopilot combination to a disturbance in roll.

Roll-simulator tests were conducted on the spring-system autopilot in order to determine its value as a possible means of pilotless-aircraft stabilization. The preference for the spring-system autopilot in these tests was mainly due to the limit set on the maximum servo displacement when the loose-link system was used. The values of the aerodynamic parameters used for setting the roll-simulator constants in the initial phase of this investigation were as follows:

L_{δ_a}, foot-pounds per radian	407
$L_{\dot{\phi}}$, foot-pounds per radian per second	-37.67
I_x, slug-feet^2	6.95

These values were obtained from the wind-tunnel data at Mach number 0.6 for the test vehicle of reference 4.

A frequency-response analysis of the spring-system autopilot for oscillating-table amplitudes of ±1.18°, ±2.92°, and ±6.82°, based on the foregoing values of L_{δ_a}, $L_{\dot{\phi}}$, and I_x and the assumption that $\frac{1}{2}$ inch of servo travel is equivalent to 20° total aileron deflection, is presented in the form of Nyquist diagrams in figure 12. The Nyquist method of frequency-response analysis and the criterions for stability are outlined in references 5 and 6. An examination of the Nyquist plots indicates that an unstable oscillation should occur between an amplitude of ±2.92° and ±1.18° because neutral stability exists at approximately ±2.92°, and at ±1.18° the Nyquist curve encloses the critical

point (-1, -180°). However, the results of the roll-simulator tests employing these same conditions did not indicate that an unstable oscillation existed but that the response of the autopilot-aircraft combination to a disturbance in roll was highly damped. A possible explanation for the discrepancy in the results of the two methods of analysis is that the method of evaluating the oscillating-table data, which is based on approximating the servo response with an equivalent sine wave, may not be valid when the servo response differs from a sine wave to the extent that it does with the spring-system autopilot at an oscillating-table amplitude of approximately ±3°. These results give an indication of what can be expected when using a linear method of analysis such as the Nyquist method for a nonlinear system.

Further roll-simulator tests were conducted for other values of $L\delta_a$ and $L\dot{\phi}$. An examination of the results of these tests, which are presented in table I, indicates that the autopilot-aircraft combination tends to become unstable as the value of $L\delta_a$ increases or as the value of $L\dot{\phi}$ decreases; thus, the range in which the frontlash autopilot could be used as a possible means of pilotless-aircraft stabilization is limited. At values of $L\delta_a = 1063$ and $L\dot{\phi} = -38$, the stability is marginal, as is indicated by the low value (0.023) of the stability coefficient. The transient response of the simulator cradle damped to an erratic ±1.5° oscillation after 3.4 seconds. This steady-state oscillation stopped after 8.5 seconds had elapsed, but a slight outside disturbance would cause it to continue. This type of instability was predicted for an $L\delta_a$ of 407 foot-pounds per radian, based on the Nyquist diagrams, and the probable reason for its occurring at the higher value of $L\delta_a$ is explained in the preceding paragraph.

A comparison of the calculated transient response of a proportional autopilot having a control-gearing ratio of 2° total aileron deflection per degree angle of bank (reference 4) with the response of the spring-system autopilot to a 10° displacement of the roll-simulator cradle, which gave a servo displacement of approximately $\frac{1}{2}$ inch, is given in figure 13. Comparing figures 13(a) and 13(b) on the basis of holding the value of $L\delta_a$ constant while varying $L\dot{\phi}$ indicates that the effect of aerodynamic damping on the response time is not as pronounced with the use of the frontlash autopilot. The principal reason for the more rapid response time at the higher values of $L\dot{\phi}$ with the nonlinear autopilot is that the servo receives a stronger initial signal due to the movement of the jet pickoffs. It is also apparent that the response of the frontlash autopilot does not become as oscillatory as the response of the proportional autopilot with decreasing $L\dot{\phi}$ in the range investigated. Comparing figures 13(a) and 13(c) on the basis of increasing $L\delta_a$ for the same value of $L\dot{\phi}$ indicates that the

nonlinearities of the frontlash system have magnified the amplitude of the transient oscillations.

Figure 14 is a presentation of the roll-simulator results giving the degree of stability as a function of the aerodynamic parameters. The degree of stability is determined by evaluating the stability-coefficient equation shown as an inset at the top of figure 14. Lines of constant values of stability coefficient are presented as plots of $L\dot{\phi}/I_X$ against $L\delta_a/I_X$. When the values of these two ratios are known, it is possible to determine the type of transient response and the degree of stability that will be obtained with the use of the frontlash autopilot. The region of high values of $L\delta_a/I_X$ to the right of the SC = 0 line represents unstable divergent response, a point falling on or near the SC = 0 line represents neutral stability, the region between SC = 0.3 and SC = 1 represents stable transient response, and the region to the left of SC = 1 represents stable but overdamped transient response. From this figure it can be seen that, for the same value of $L\dot{\phi}/I_X$, stabilization of pilotless aircraft with values of $L\delta_a/I_X$ above 130 is more critical with the frontlash autopilot because in the region shown there is a rapid transition from a stable to an unstable transient response due to an increase in $L\delta_a/I_X$. The accuracy of the upper portion of the lines of constant stability coefficient is limited because the electrical output of the roll simulator becomes nonlinear in this range, thus causing increased inaccuracies in simulation of the aerodynamic parameters. The over-all accuracy of the roll-simulator results is estimated to be within 20 percent.

CONCLUSIONS

The two automatic-pilot systems tested in this investigation operate on a nonlinear principle whereby a dead spot is incorporated in the servomotor feedback linkage. The conclusions arrived at as a result of the tests conducted on these automatic-pilot systems are as follows:

Both of the methods of applying the frontlash principle improve the phase response of the servomotor in a manner similar to that which would be obtained with the use of a rate gyroscope. However, the servomotor travel resulting from a given gyroscope displacement is decreased when the frontlash feedback linkage is used.

The results of the roll-simulator tests indicate that the frontlash automatic pilot has promise as a pilotless-aircraft stabilization

system. In a certain range of simulated aerodynamic parameters, it is shown that the nonlinear frontlash automatic pilot has a higher degree of stability than a comparable linear system. However, the transition from a stable to an unstable autopilot-aircraft combination appears to be more rapid with the nonlinear system.

The results and applications of the roll-simulator investigation also indicate that there is a need for study of the methods for handling nonlinear components in an automatic-pilot system. Although it may be useful, the application of linear methods to systems having nonlinear components will not usually give the accuracy required for the evaluation of an automatic pilot.

Langley Aeronautical Laboratory,
National Advisory Committee for Aeronautics,
Langley Field, Va., July 7, 1949.

REFERENCES

1. Hoch, Hans: Directional Stability by Means of a Limit Switch in the Neutralizing Control. Translation No. F-TS-559-RE, Air Materiel Command, Army Air Forces, June 14, 1946.

2. Seamans, Robert C., Jr., Bromberg, Benjamin G., and Payne, L. E.: Application of the Performance Operator to Aircraft Automatic Control. Jour. Aero. Sci., vol. 15, no. 9, Sept. 1948, pp. 535-555.

3. Greenberg, Harry: Frequency-Response Method for Determination of Dynamic Stability Characteristics of Airplanes With Automatic Controls. NACA Rep. 882, 1947.

4. Teitelbaum, Jerome M., and Seaberg, Ernest C.: An Experimental Investigation of a Gyro-Actuated Roll Control System Installed in a Subsonic Test Vehicle. NACA RM L9B24a, 1949.

5. James, Hubert M., Nichols, Nathaniel B., and Phillips, Ralph S.: Theory of Servomechanisms. McGraw-Hill Book Co., Inc., 1947.

6. Hall, Albert C.: The Analysis and Synthesis of Linear Servomechanisms. The Technology Press, M.I.T., 1943.

TABLE I

RESULTS OF ROLL-SIMULATOR TESTS FOR VARIOUS VALUES OF L_{δ_a} AND $L_{\dot{\phi}}$

[Results based on transient response to 10° displacement in roll]

L_{δ_a} (ft-lb/rad)	$L_{\dot{\phi}}$ (ft-lb/rad/sec)	I_x (slug-ft^2)	Stability coefficient,[a] SC	Time to damp to 0° (sec)	Amplitude of oscillation (deg)	Frequency of oscillation (cps)
407	-29	6.95	0.71	0.68	-----	----
776	-29	6.95	.199	1.33	-----	1.59
890	-29	6.95	.167	3.14	-----	2.07
993	-29	6.95	0	----	±18	1.87
1063	-29	6.95	0	----	±26	1.62
407	-38	6.95	.729	.55	-----	----
619	-38	6.95	.460	.60	-----	----
776	-38	6.95	.307	1.10	-----	1.85
1063	-38	6.95	.023	8.50	±1.5	2.27
1170	-38	6.95	0	----	±19	2.18
407	-56	6.95	1	.26	-----	----
776	-56	6.95	.373	.60	-----	----
1063	-56	6.95	.196	2.50	-----	2.17
1066	-56	6.95	.122	3.47	-----	2.29
1108	-56	6.95	0	----	±14.5	2.28
1254	-56	6.95	0	----	±20	2.17
407	-69	6.95	1	.24	-----	----
776	-69	6.95	.600	.58	-----	----
1063	-69	6.95	.198	1.4	-----	2.17
1141	-69	6.95	.087	3.70	-----	2.56
1254	-69	6.95	0	----	±19	2.27
407	-75	6.95	1	.23	-----	----
776	-75	6.95	.605	.58	-----	----
1063	-75	6.95	.350	1.10	-----	2.50
1170	-75	6.95	.167	3.63	-----	2.65
1254	-75	6.95	0	----	±14	2.58

[a]The value of this coefficient is unity for a highly damped (dead-beat) oscillation, zero for a steady-state oscillation, and negative for an unstable oscillation.

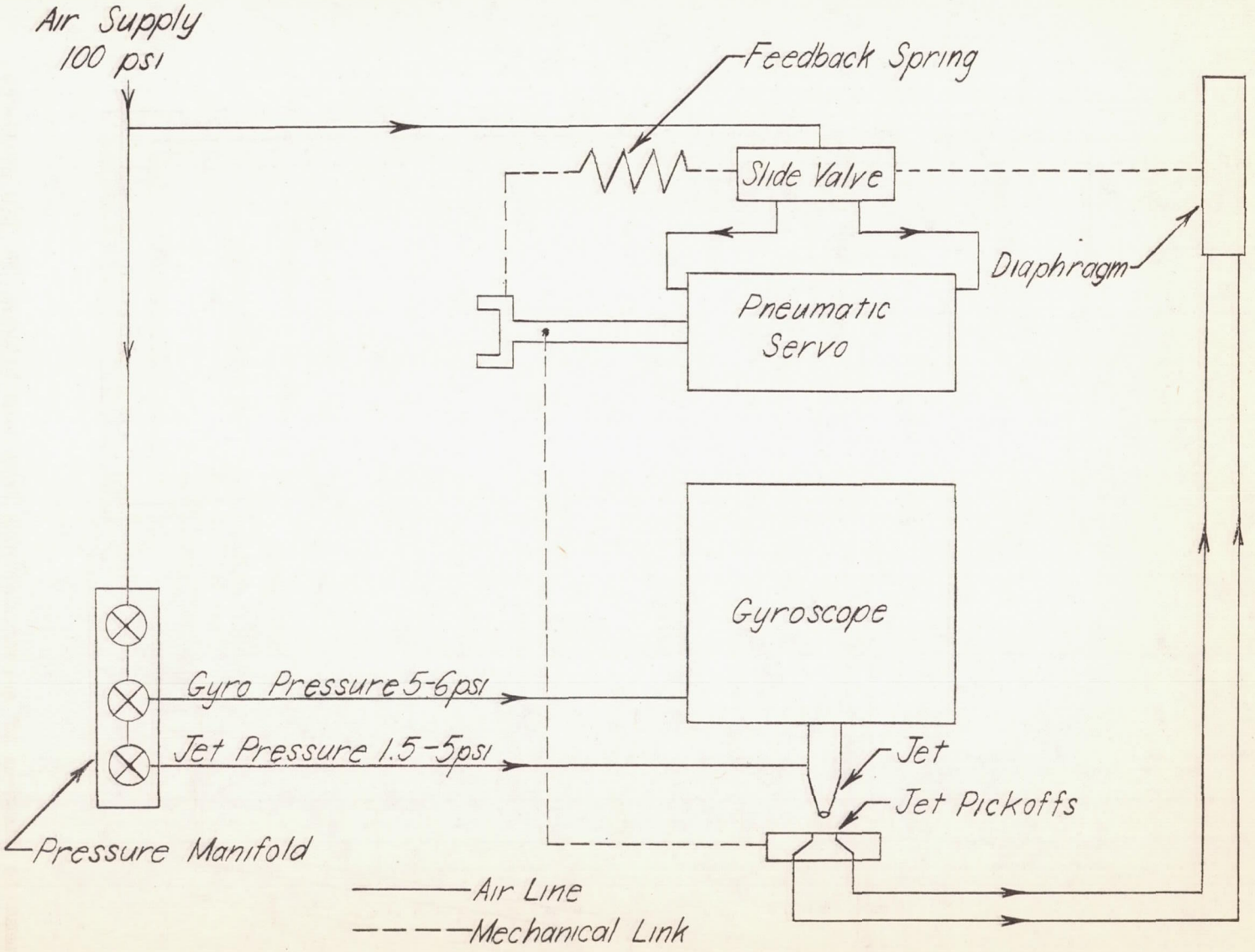

Figure 1.- Block diagram of frontlash autopilot system.

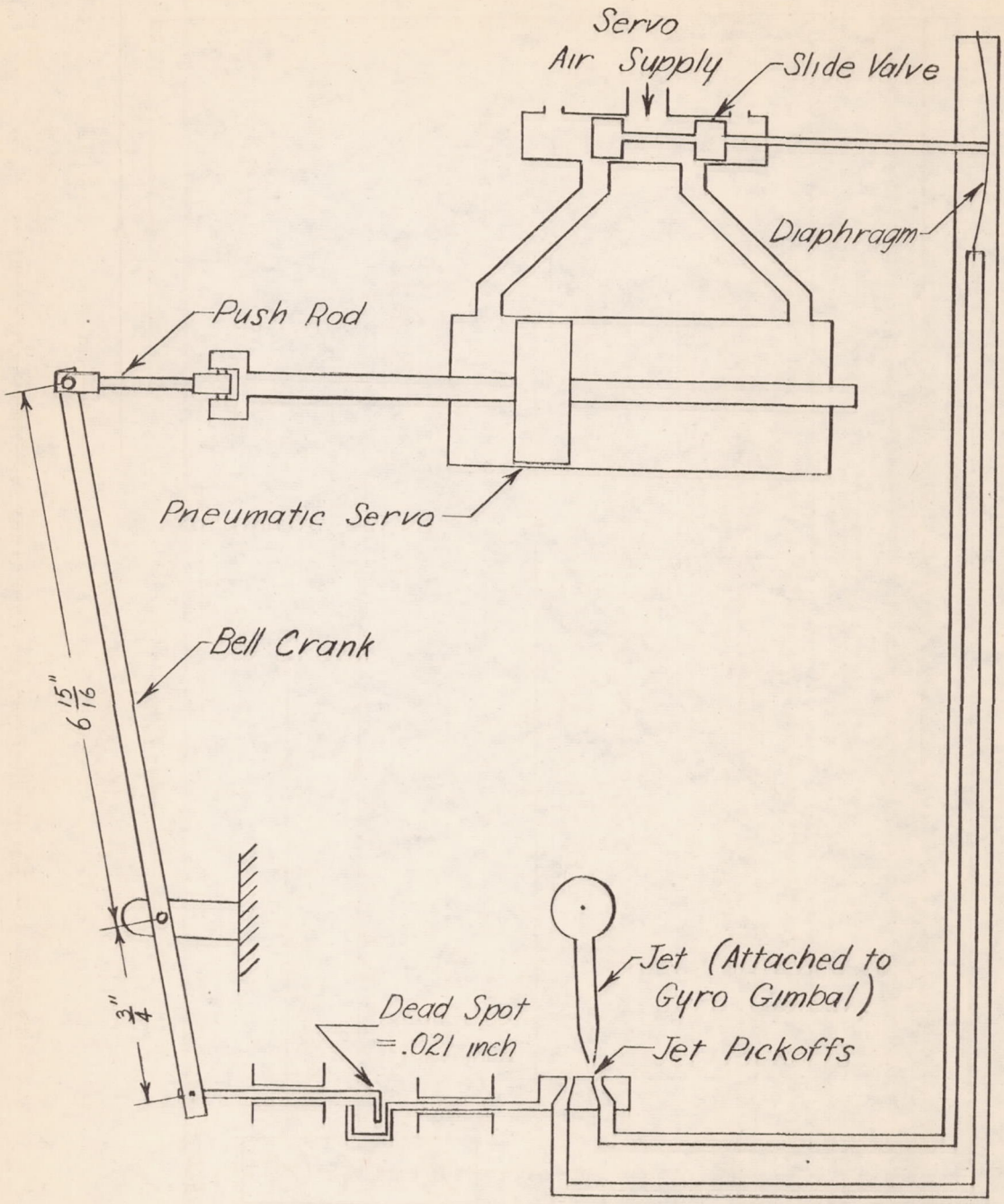

(a) Schematic diagram of servomotor and feedback linkage to jet pickoffs showing loose link containing dead spot.

Figure 2.- Loose-link system.

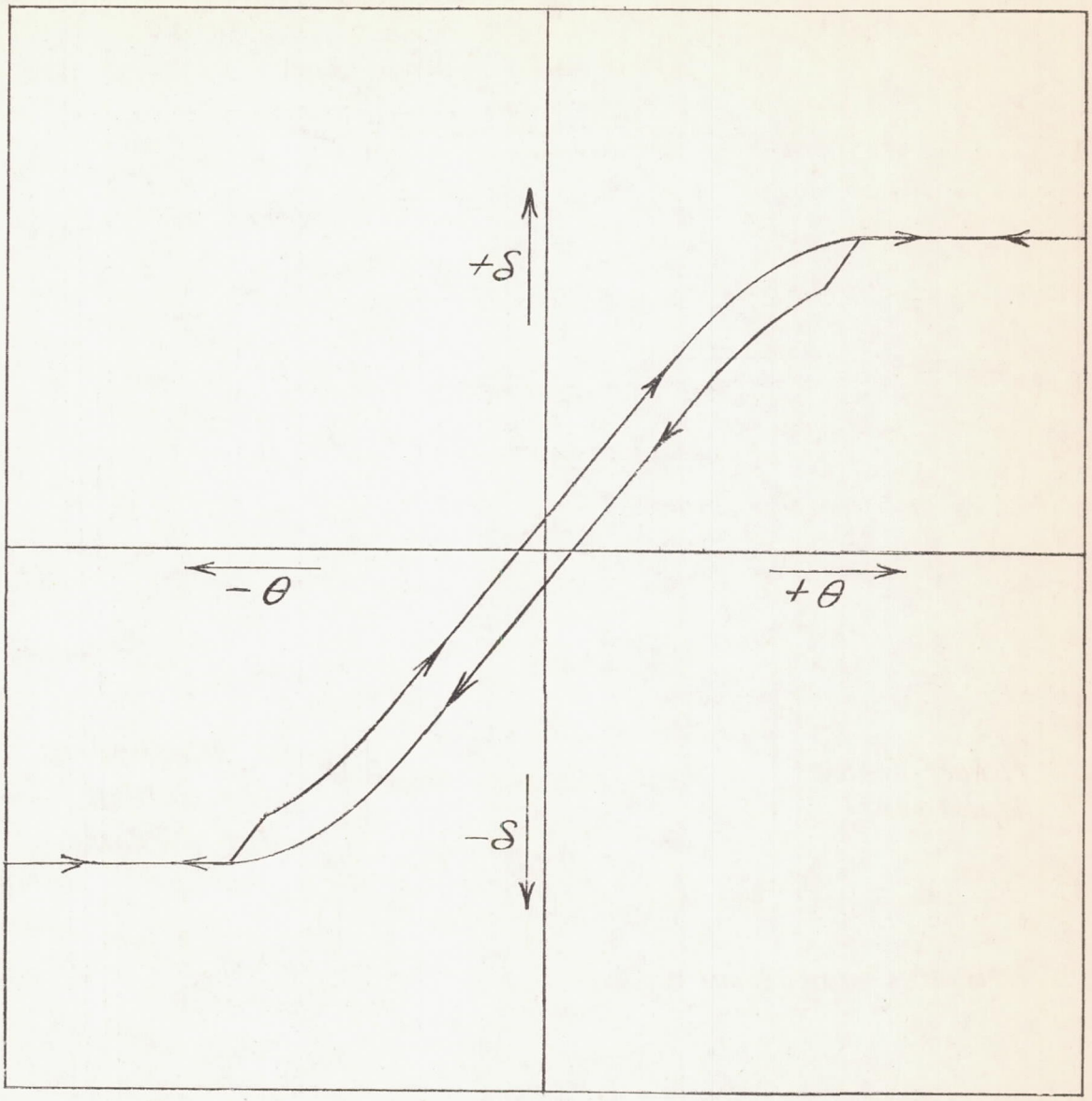

(b) Schematic representation of the static variation of servomotor position with oscillating-table displacement for the loose-link system.

Figure 2.- Concluded.

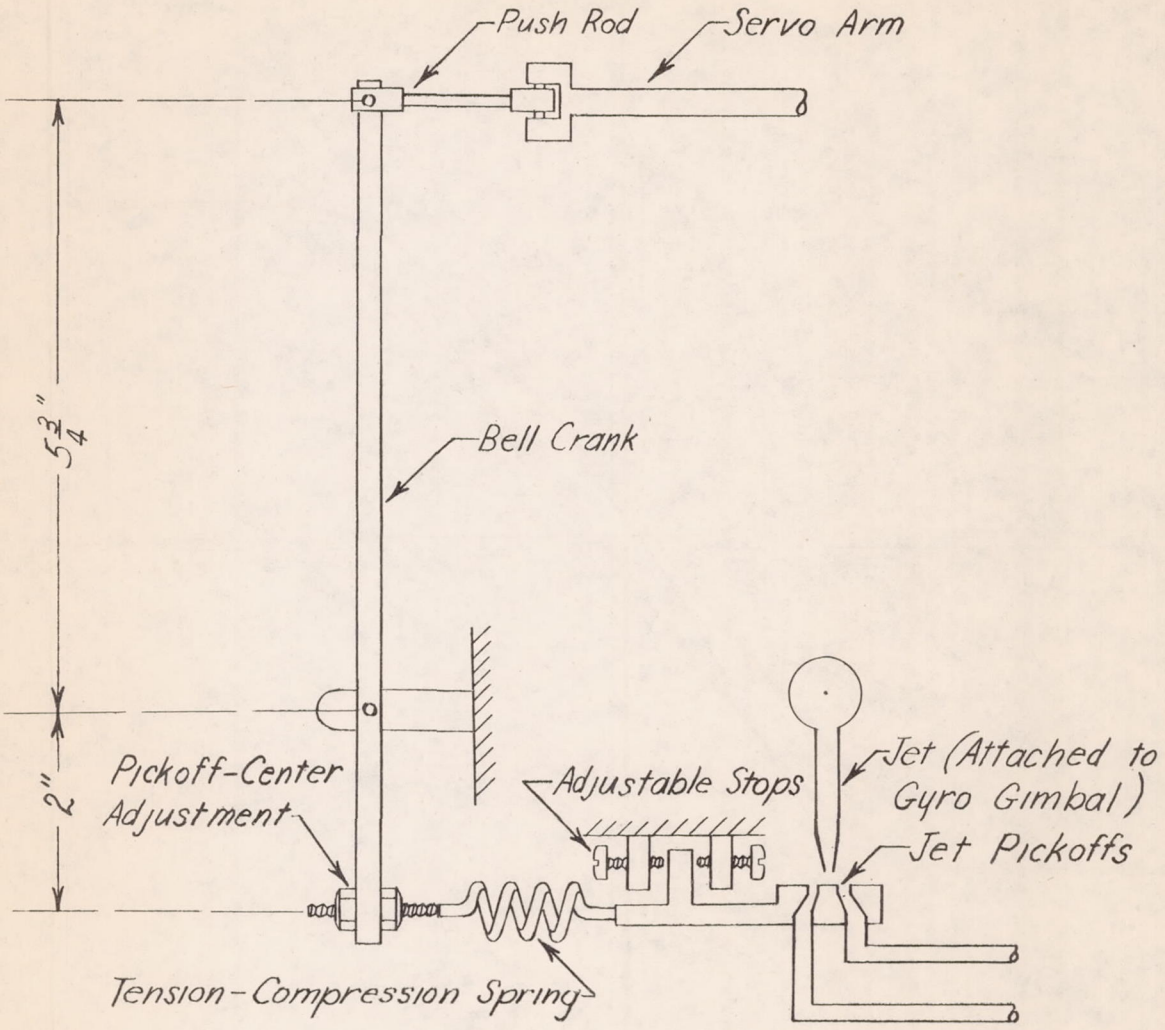

(a) Schematic diagram of servomotor feedback linkage to jet pickoffs showing tension-compression spring and adjustable stops for setting dead spot.

Figure 3.- Spring system.

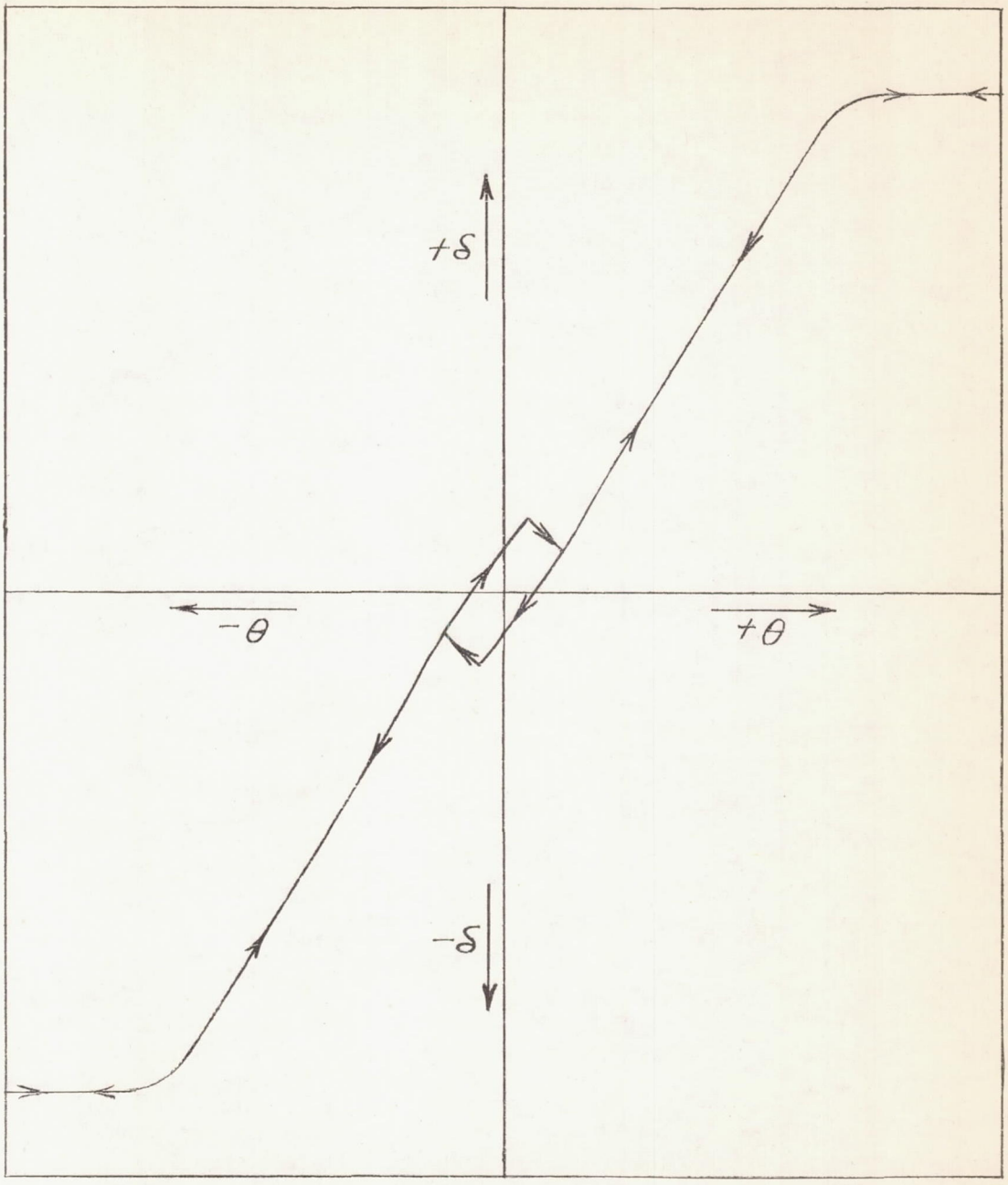

(b) Schematic representation of the static variation of servomotor position with oscillating-table displacement for the spring system.

Figure 3.- Concluded.

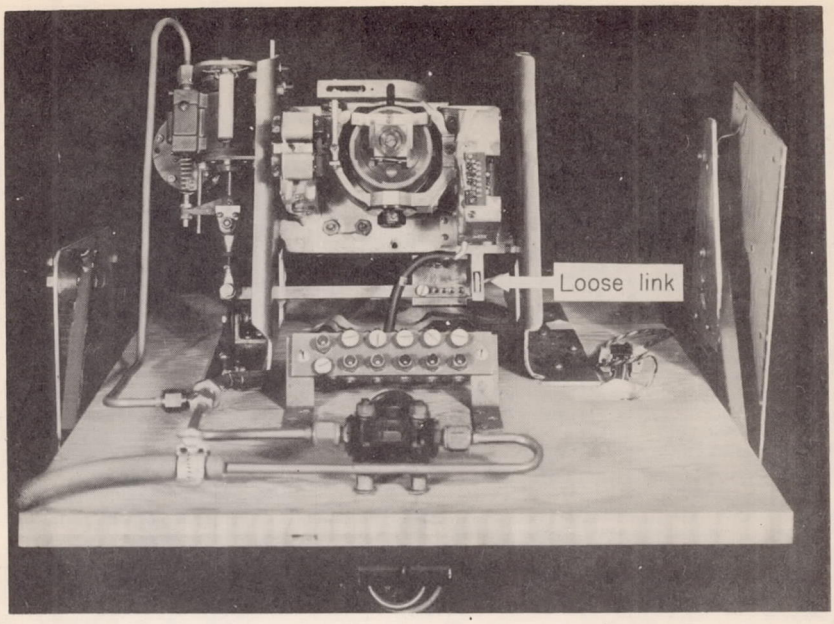

(a) Loose link containing dead spot in servomotor feedback linkage.

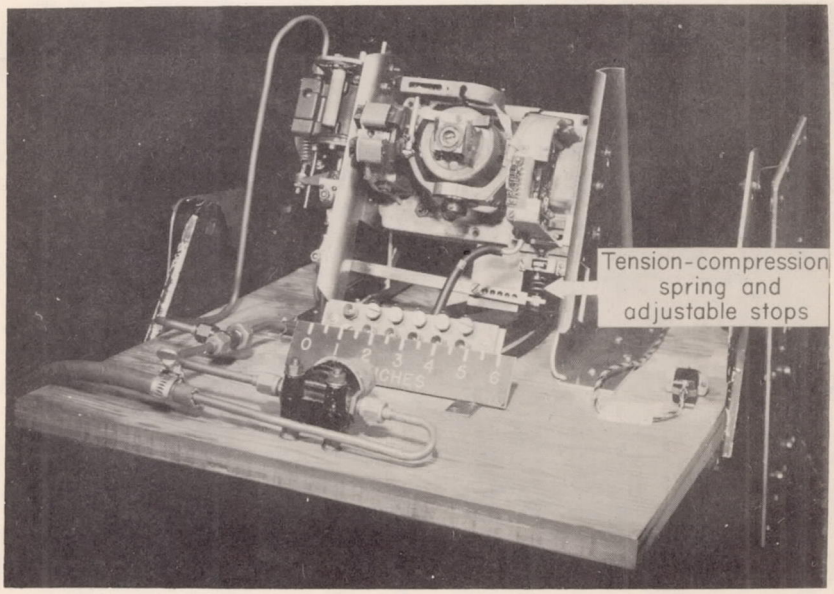

L-60576

(b) Tension-compression spring and adjustable stops in servomotor feedback linkage.

Figure 4.- Oscillating-table installations of the two frontlash autopilot systems.

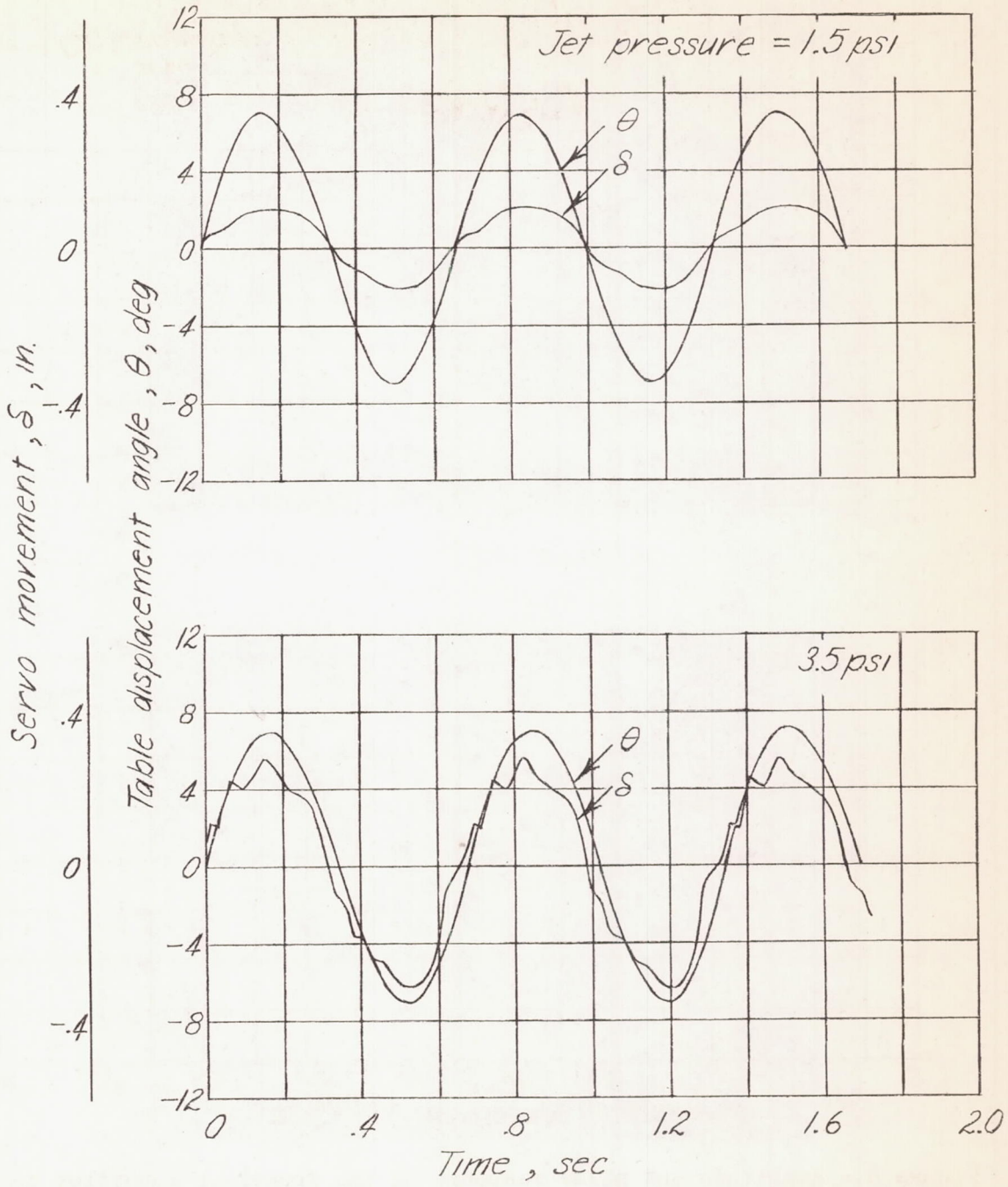

Figure 5.- Effect of varying jet pressure on the response of the front-lash autopilot to a table oscillation of ±7° at approximately 1.5 cycles per second with a dead spot of 0.021 inch in the jet-pickoff feedback linkage.

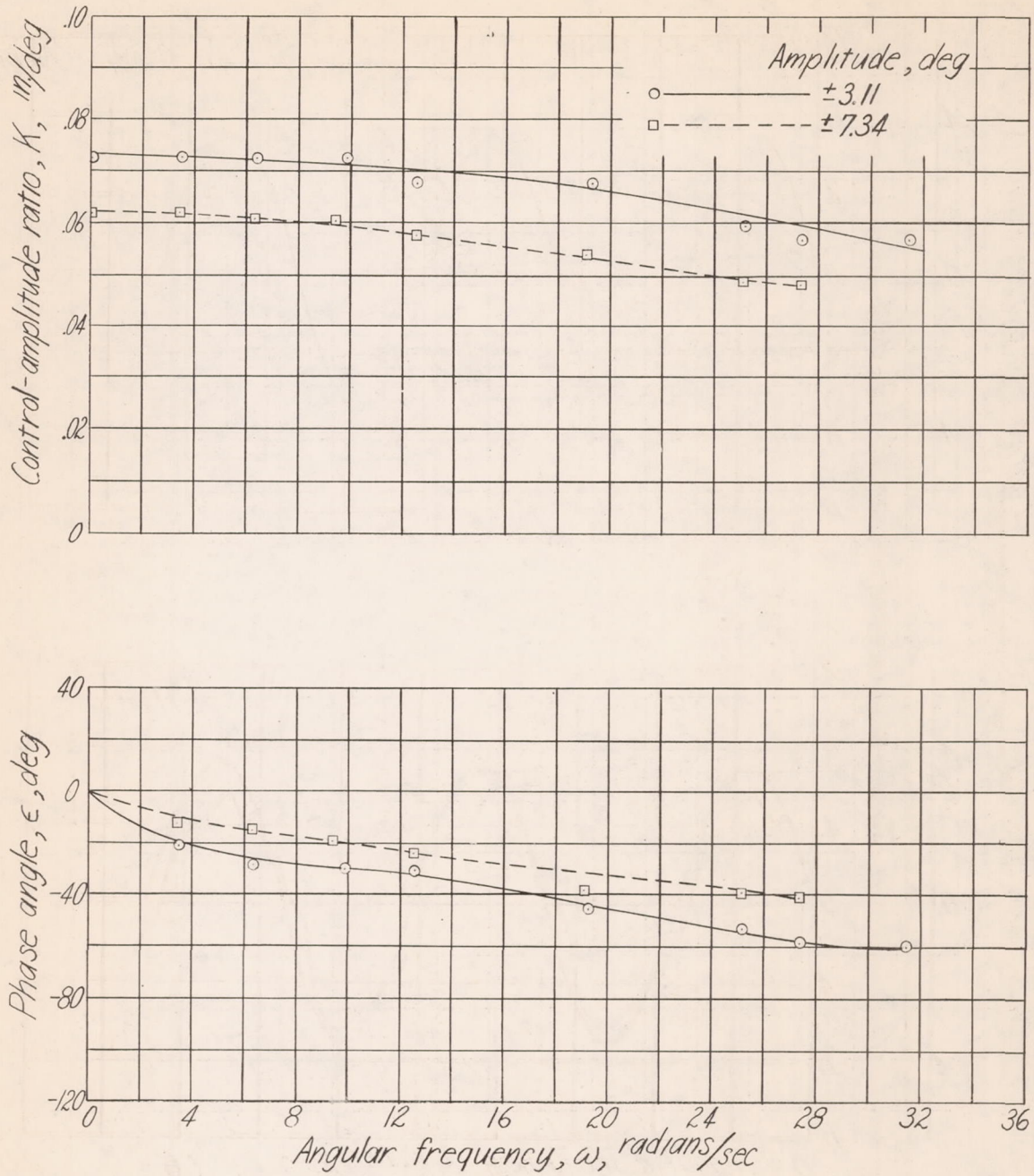

Figure 6.- Amplitude and phase response of the frontlash autopilot to table-oscillation amplitudes of ±3.11° and ±7.34° with fixed jet pickoffs and a jet pressure of 3.5 psi.

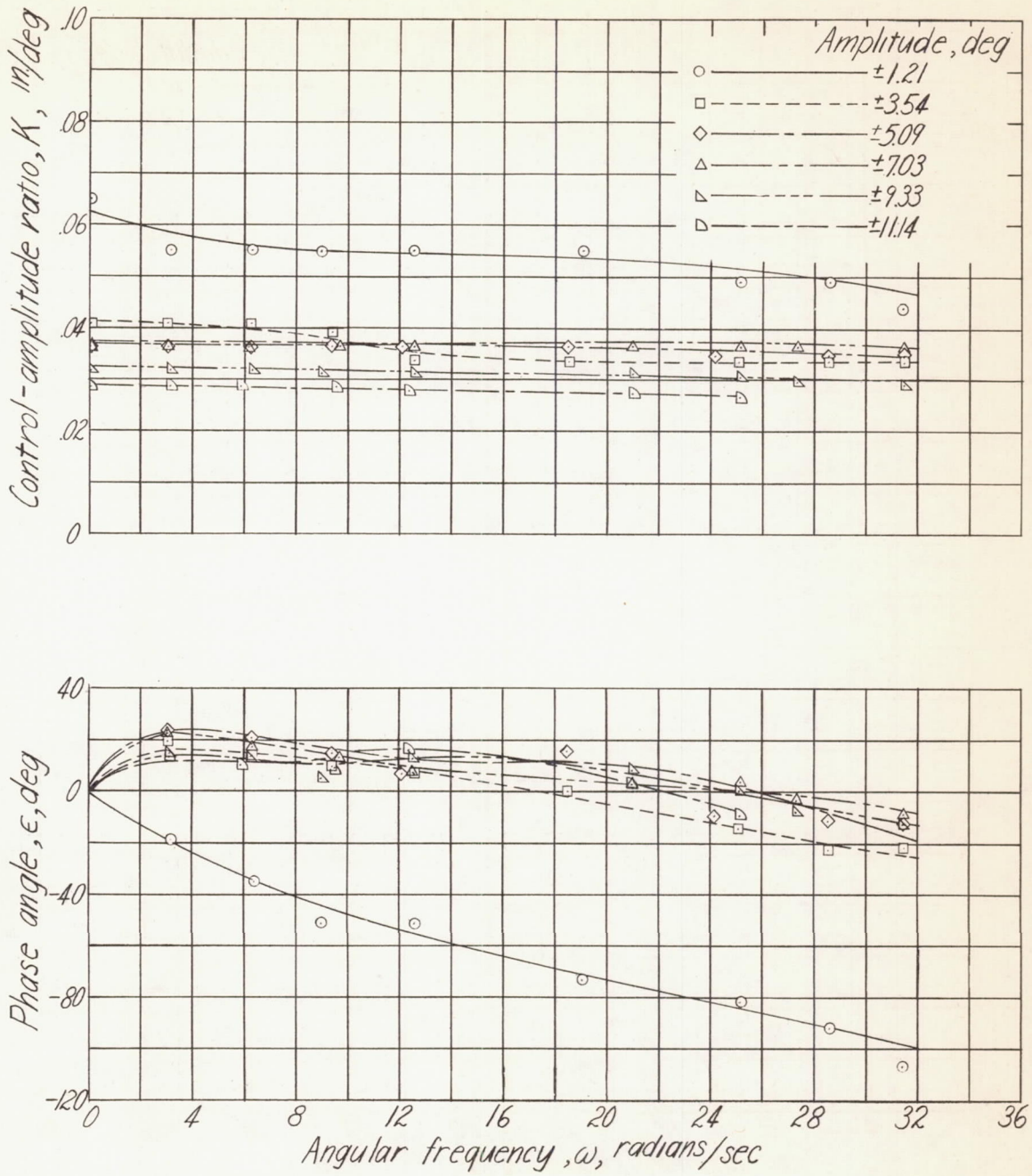

Figure 7.- Amplitude and phase response of the frontlash autopilot to various table-oscillation amplitudes using a dead spot of 0.021 inch and a jet pressure of 3.5 psi.

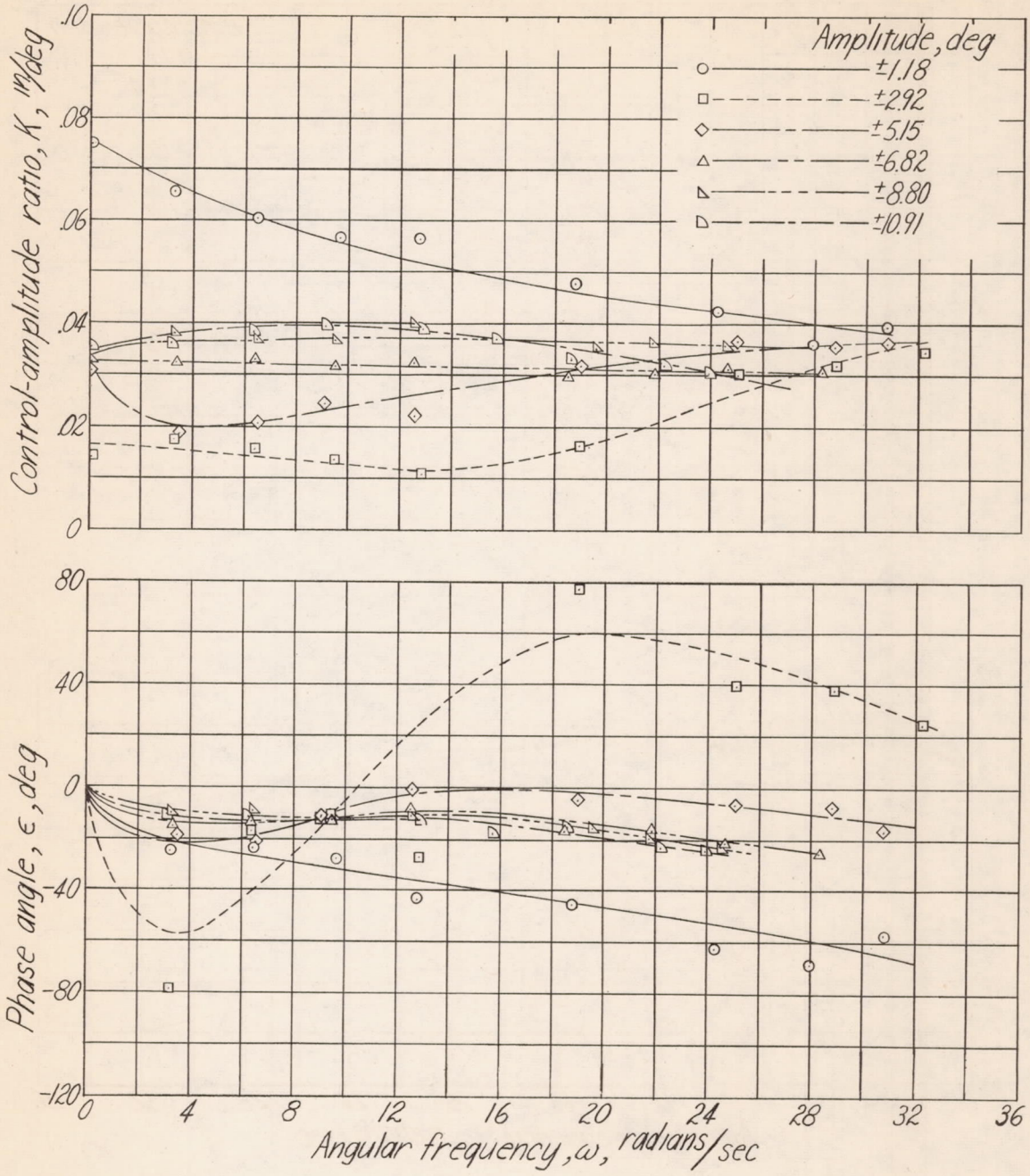

Figure 8.- Amplitude and phase response of frontlash autopilot with spring in jet-pickoff feedback linkage to various table-oscillation amplitudes using a dead spot of 0.016 inch and a jet pressure of 3 psi.

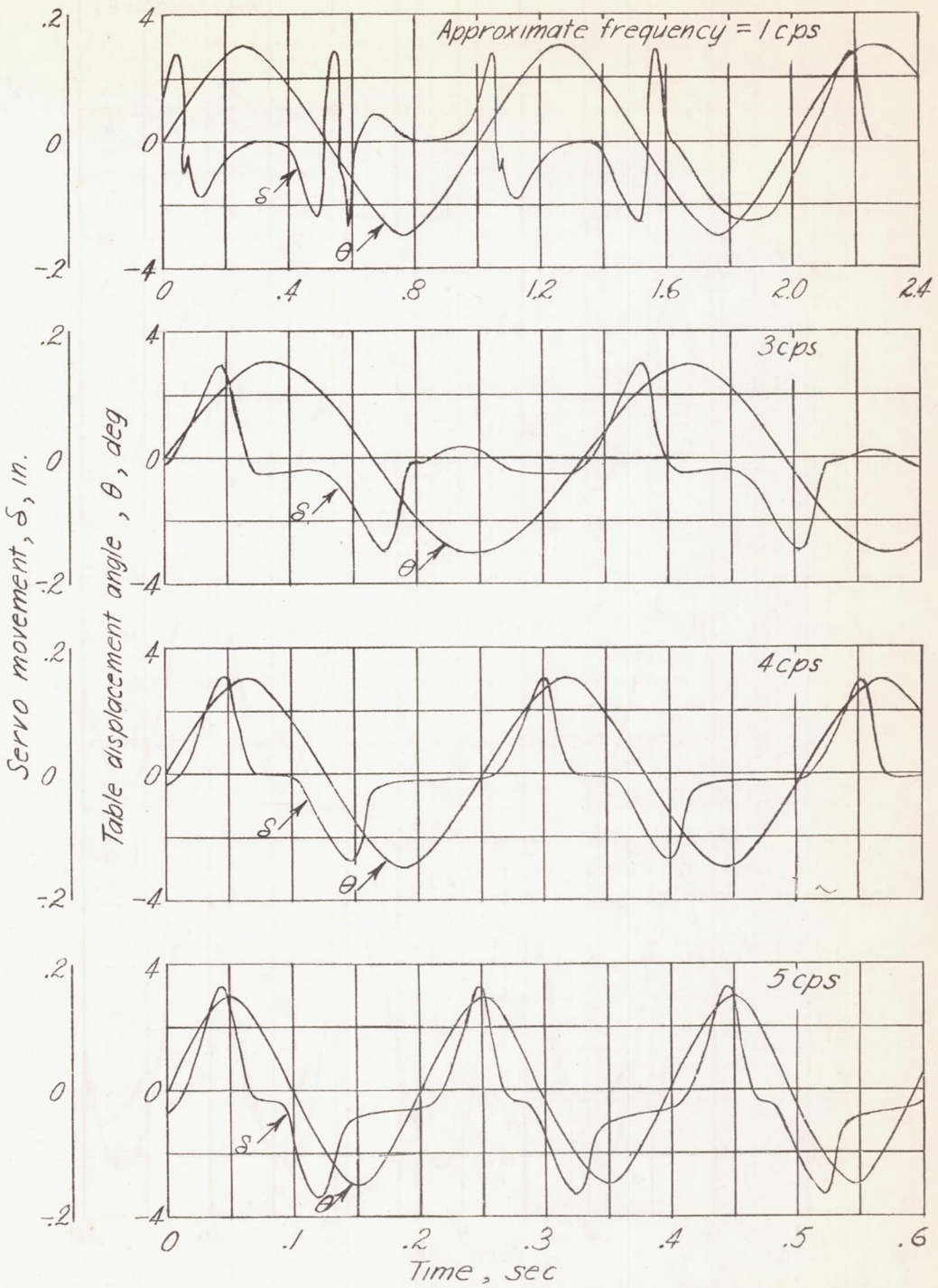

Figure 9.- Type of response obtained from frontlash autopilot with spring in jet-pickoff feedback linkage at various frequencies, at a table-oscillation amplitude of ±2.92°, jet pressure of 3 psi, and dead spot of 0.016 inch.

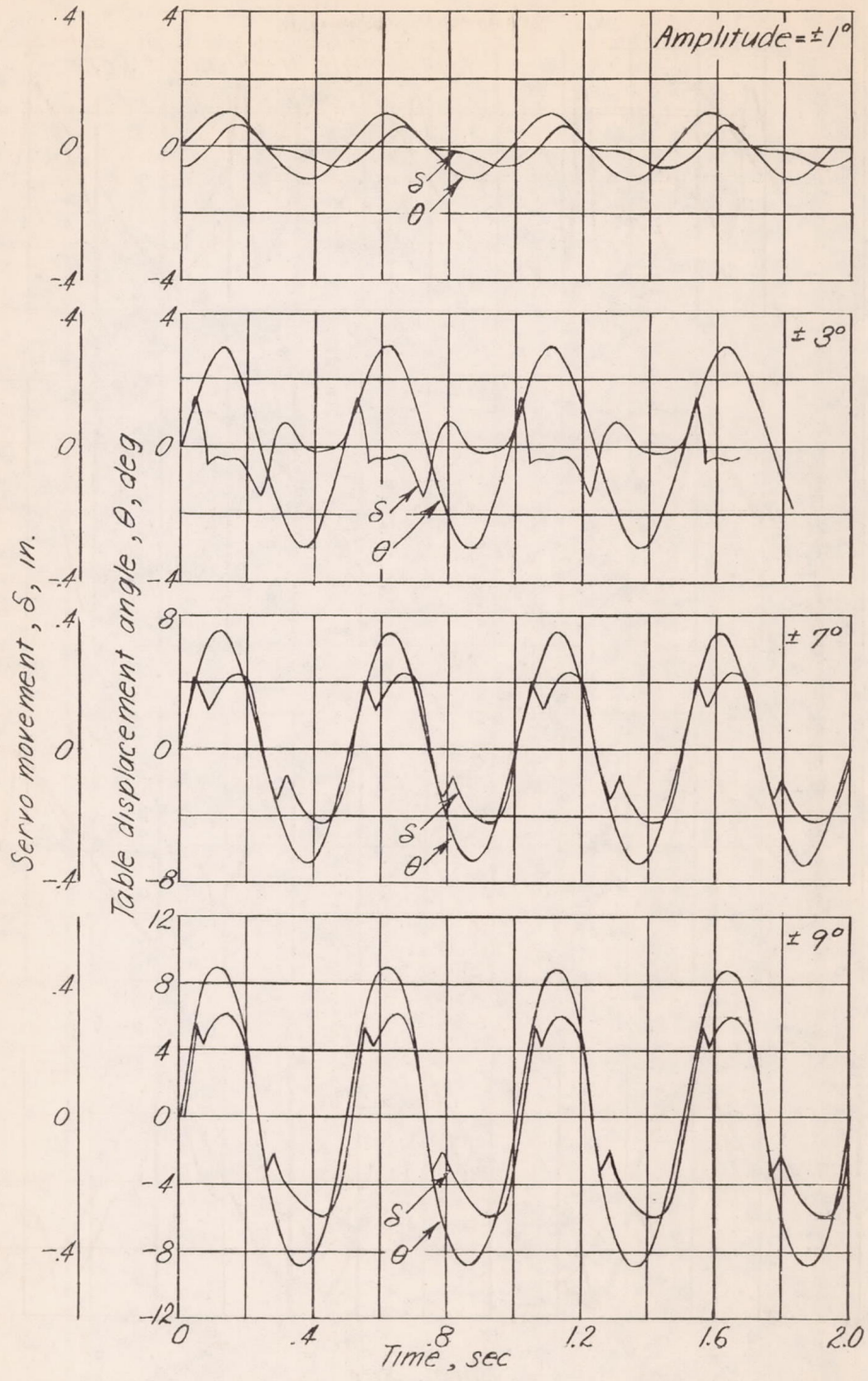

Figure 10.- Type of response obtained from frontlash autopilot with a spring in jet-pickoff feedback linkage of various amplitudes of table oscillation, at a frequency of approximately 2 cycles per second, jet pressure of 3 psi, and dead spot of 0.016 inch.

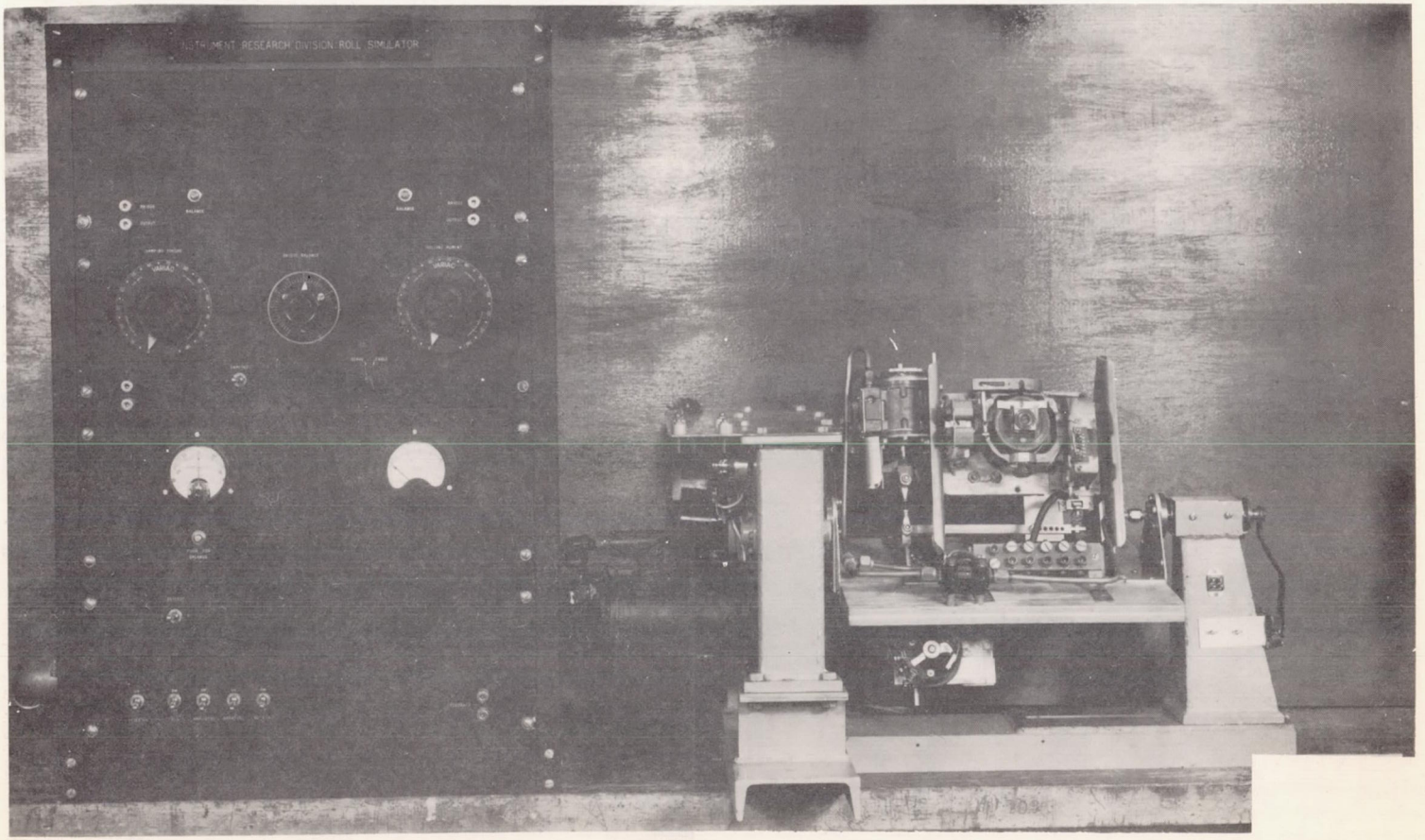

Figure 11.- Roll-simulator installation of the frontlash autopilot with tension-compression spring and adjustable stops in the servomotor feedback linkage.

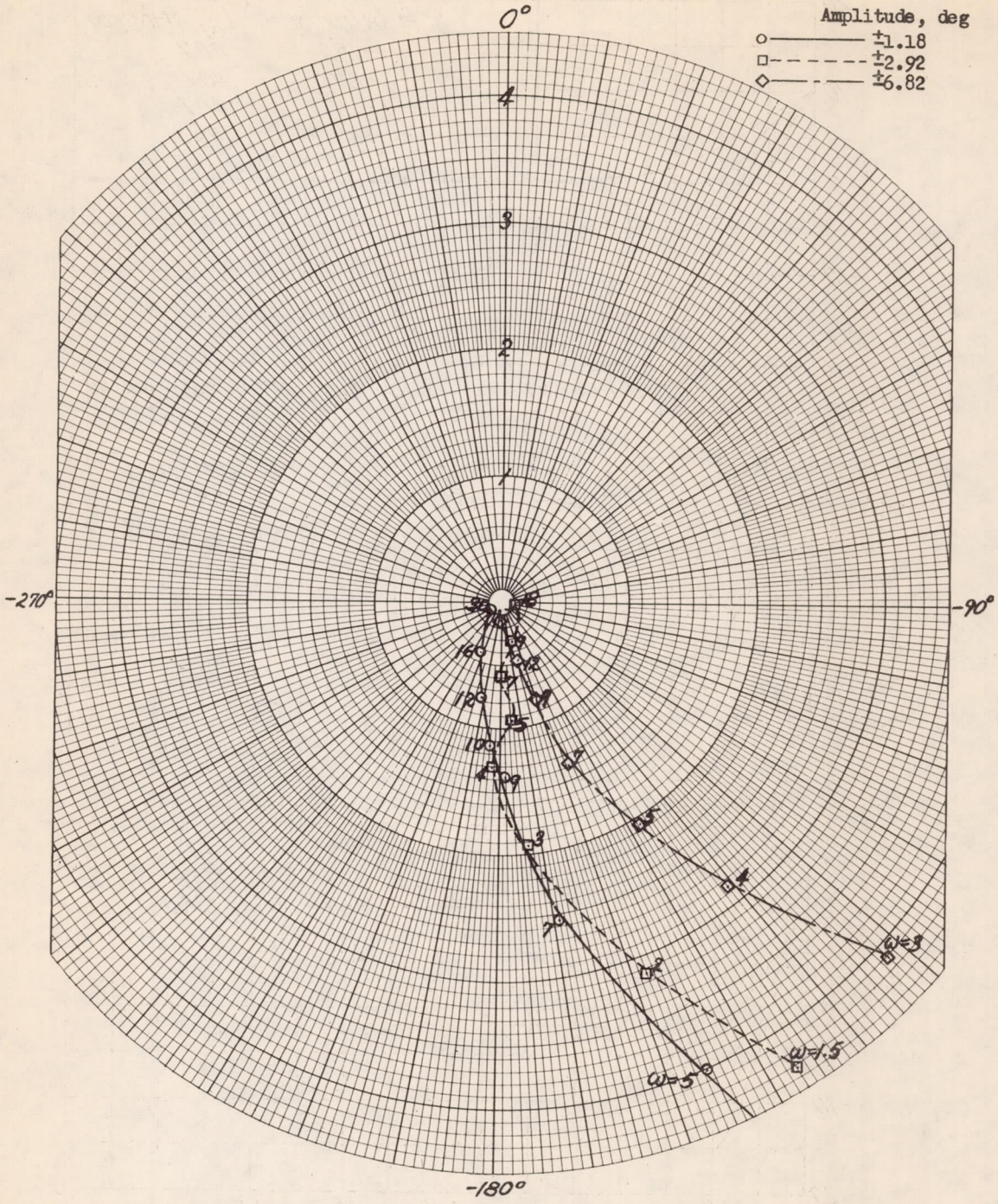

Figure 12.- Nyquist diagrams for lateral roll oscillations of ±1.18°, ±2.92°, and ±6.82° based on test vehicle with aerodynamic derivatives of $L\delta_a$ = 407 ft-lb/radian, $L\dot{\phi}$ = -37.67 ft-lb/radian/sec, and I_x = 6.95 slug-ft^2.

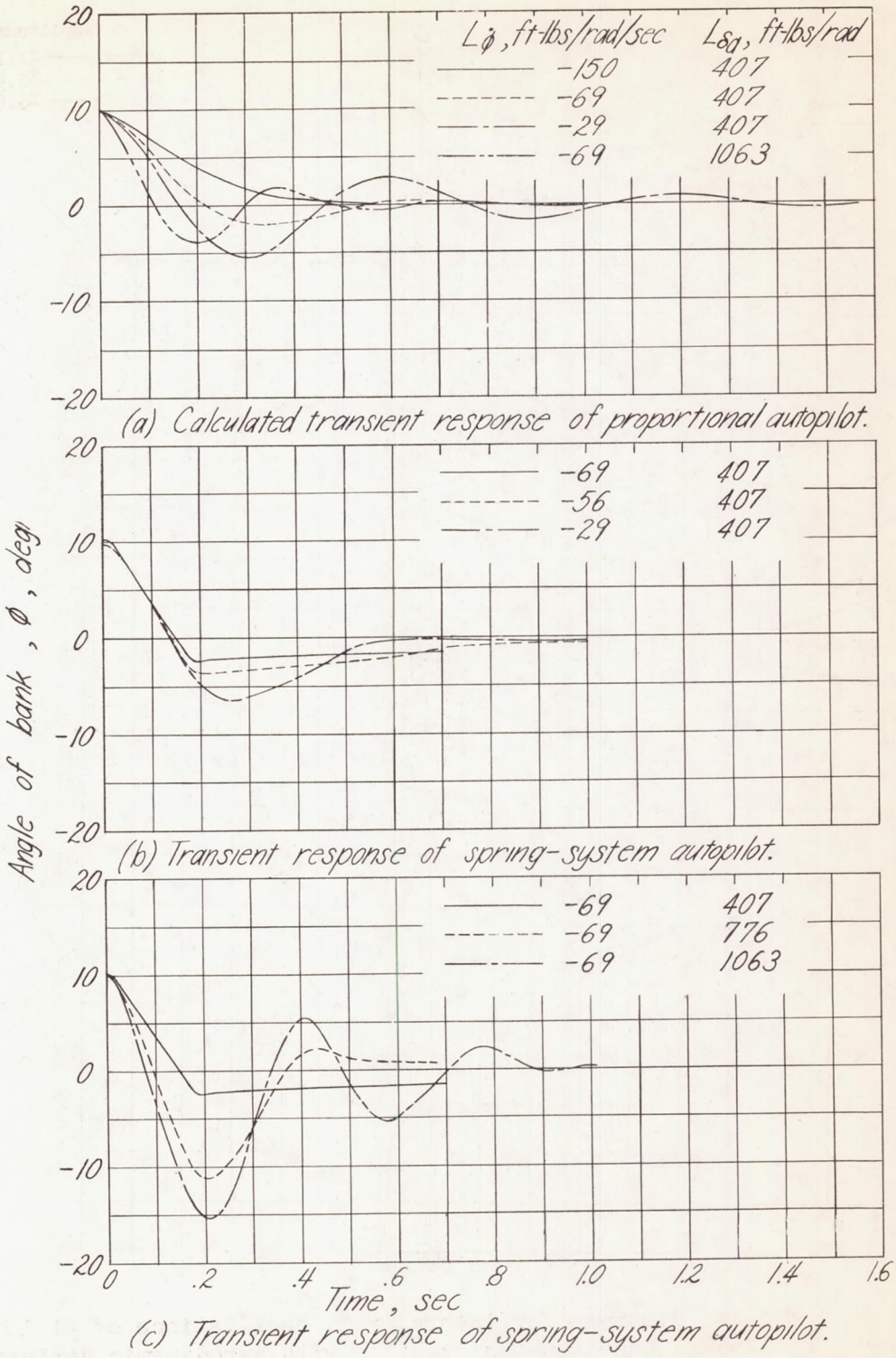

Figure 13.- Comparison of calculated transient response of proportional autopilot with the response of the spring-system autopilot to a 10° displacement of the roll-simulator cradle. I_x = 6.95 slug-ft^2.

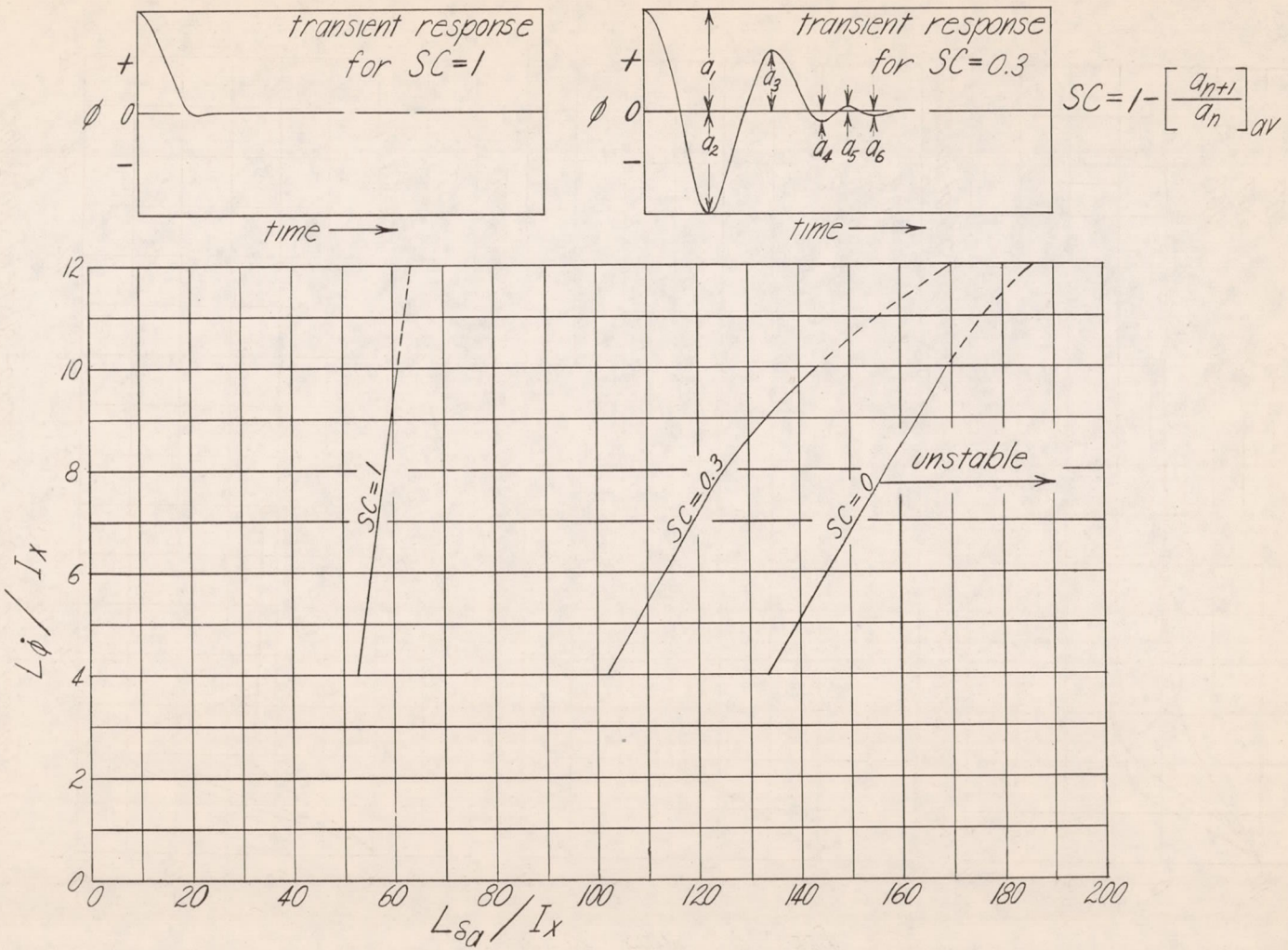

Figure 14.- Results of roll-simulator tests on spring-system autopilot giving the degree of stability as a function of the aerodynamic parameters.